On-Body Adhesive-Bandage-Like Antenna for Wireless Medical Telemetry Service

Yu-Jen Chi, *Student Member, IEEE*, and Fu-Chiarng Chen, *Member, IEEE*

***Abstract*—This paper presents a novel planar, via-free, printed antenna for wireless medical telemetry service (WMTS). The antenna structure is simple and looks like an adhesive bandage, and can be placed on human tissue. Depending on the application, the antenna can be used as a standalone antenna when it is fed by a coaxial cable, or it can be integrated with a single-chip sensor, with the chip placed in the center. Antenna parameters, such as reflection coefficients, radiation patterns, radiation efficiency, and the specific absorption rate, were evaluated in various scenarios to validate the proposed design. The measured radiation efficiency of the proposed adhesive-bandage-like antenna was 89.5% in free space and 44.7% when mounted on tissue-equivalent phantom. The antenna also retained its broad side radiation characteristics when it was bent at 90°. The proposed antenna is a favorable candidate for use in wireless body area networks (WBANs). This paper presents the detailed design considerations of the proposed antenna.**

***Index Terms*—Adhesive-bandage-like antenna, deformation, on-body, wireless body area networks (WBANs), wireless medical telemetry service (WMTS).**

I. Introduction

WIRELESS body area networks (WBANs) were developed in 1995 and are specifically designed for wearable computing device applications. With the rapid development of wireless communication and low-power integrated circuits, wearable computing devices can now be worn for long periods and can be used to measure body signals, such as electrocardiography (ECG), electroencephalography (EEG), electromyography (EMG), pulse oximeter, and body temperature data. These signals can be transmitted to a central process node (CPN) through a wireless network, allowing medical officers to access the data and provide clinical health care from long distances. These promising applications have transformed wireless sensor networks into a new generation of networks that have improved the quality of medical services and health care, allowing health care providers to monitor patients continuously, wirelessly, intelligently, and at a low cost. To gather physical information wirelessly and transmit the data to a remote CPN by using a wireless sensor node, a wireless sensor unit must be compact, have a low profile, and be stable during operation. The main challenge in designing antennas for wireless sensor node applications is that general requirements for WBANs mean that antennas must be planar and be printed on circuit boards. Human tissue is a lossy material, therefore antennas operating near the body demonstrate frequency shifts, low-antenna gain, and radiation pattern distortion. To overcome these problems, antennas should also exhibit relatively low fringing fields in body tissue to reduce detuning and the specific absorption rate (SAR). In addition, to maintain data transmission reliability, antennas should have radiation patterns that are oriented away from the body.

On-body channel characteristics and the influence of the body on antenna performance have been investigated [1]–[3]. Several antenna designs that are suitable for WBANs have also been proposed [4]–[21]. [4] and [5] presented wearable Yagi antennas for on-body communication applications. [6]–[9] examined small cavity slot antennas and compact ultra-wideband antennas. However, these compact designs require three-dimensional (3D) layouts and have a thick antenna height of 4 mm to 10 mm. Flexible antenna designs, such as textile antennas or antennas printed on fabric substrates, have been proposed [10]–[16], and the bending effect has also been studied. However, these antennas require vertical probe feeding schemes or vias in the antenna structures. Metamaterial antenna designs for on-body communications have also been published [17], [18]. The antenna in [17] consisted of periodically arrayed composite right/left-handed unit cells to form a zeroth-order resonant antenna. At the zero phase constant, the resonant condition does not depend on the physical dimension of the antenna, but on the value of right/left-handed capacitance and inductance. This produced an electrically small antenna, the performance of which was invariant to substrate deformation. However, the antenna was based on a coplanar waveguide (CPW) structure that did not have a ground plane between the antenna and the human body, affecting the impedance matching, antenna gain, and radiation patterns through its proximity to the body tissue. [18] presented a similar structure, but it was based on a CPW ground technique. Because of the presence of a ground plane between the resonator and the body tissue, the performance was insensitive to the on-body condition. However, using chip inductors increased the fabrication complexity, and the achieved peak gain was only -7 dBi on the broad side. [19] proposed a high-efficiency, twin-slot antenna fed by a conductor-backed CPW. Most of the antenna power was directed to the broad side, and the electromagnetic field was isolated by the ground plane on the back. These characteristics made the antenna a strong candidate for on-body applications. However, the antenna was relatively large and the size of the ground plane af-

Manuscript received September 04, 2012; revised February 07, 2013; accepted February 13, 2014. Date of publication February 27, 2014; date of current version May 01, 2014. This work was supported by the National Science Council and Ministry of Economics, Taiwan, R.O.C., under Grants NSC 102-2219-E-009-002- and MOEA 99-EC-17-A-03-S1-005.

The authors are with the Department of Electrical Engineering, National Chiao Tung University, Hsinchu 30010, Taiwan (e-mail: fchen@faculty.nctu.edu.tw).

Color versions of one or more of the figures in this paper are available online at http://ieeexplore.ieee.org.

Digital Object Identifier 10.1109/TAP.2014.2308918

fected the antenna performance, making it unsuitable for integration with a wireless sensor node. [20] and [21] studied antennas printed on disposable plaster, which is a promising design for compact body-worn antennas. This paper proposes a planar, via-free, printed antenna, which looks like an adhesive bandage (also known by the generic trademark, Band-Aid) for wireless medical telemetry service (WMTS). The Federal Communications Commission (FCC) spectrum specification [22] allocates three sets of frequency bands (608–614 MHz, 1.395–1.4 GHz, and 1.427–1.432 GHz) in the United States. WMTS provide an interference-free spectrum to prevent overcrowding in the well-used industrial-science-medical (ISM) band. The proposed antenna was designed for a wireless health care monitoring system operating on the primary 1.429 to 1.4315 GHz band [23]. This antenna was mainly designed for chest-mounted wireless sensor nodes, but it can also be used in applications that require curved designs. Therefore, the radiation characteristics of antenna deformation were also investigated in this study. This paper is organized as follows. Section II describes the antenna design method and its mechanism, including the feeding method and characteristics of the virtually connected ground conductor. Section III describes the antenna deformation. Section IV provides a method for decreasing the SAR. Section V presents a summary of the experimental results, and Section VI concludes the study.

II. Antenna Design

This section describes the design of an adhesive-bandage-like planar antenna for a WBAN. Microstrip antennas are planar and easily fabricated, and they exhibit shielded ground planes on their backs, therefore the proposed design was based on a microstrip antenna. The original design of the adhesive-bandage-like antenna is shown in Fig. 1. The antenna comprised a rectangular patch and a rectangular metal ring on top of the circuit board, as well as a ground conductor on the back. A 0.8-mm-thick Duroid RT5880 dielectric substrate with a dielectric constant of 2.2 and a loss tangent of 0.0009 was used. The length of the rectangular patch was approximately a half wavelength at 1.4 GHz, and its width was 5.46 times smaller than its length. This design could be used for a standalone antenna if it was fed by a mini coaxial cable with a small diameter, or it could be integrated into an ultralow-power wireless vital signs monitoring system [24].

A. Antenna Description

The proposed antenna design was based on a microstrip patch antenna and a coplanar patch antenna (CPA) with a CPW feed line [25], [26]. Generally, conventional microstrip antennas exhibit the attractive features of being low-profile, lightweight, easily fabricated, and conformable to mounting hosts. Various methods can be used for microstrip antenna feeds, such as a coaxial feed, an inset feed, a proximity-coupled feed, and an aperture-coupled feed. However, these feeding methods require vertical feeding probes or multilayer structures, which are unsuitable for applications in small wireless biosensors. Therefore, a CPA was selected as the reference design since it is uniplanar and is easily integrated into active and passive devices. Research has shown that a CPA, which has a structure similar to that of a slot loop antenna, behaves more like a microstrip antenna [27]. Therefore, it is expected that this type of antenna can excite both TM_{01} and TM_{10} modes. To reduce the size of the patch resonator, the length of the patch resonator was decreased, and a width-to-length ratio of 5.46 was implemented.

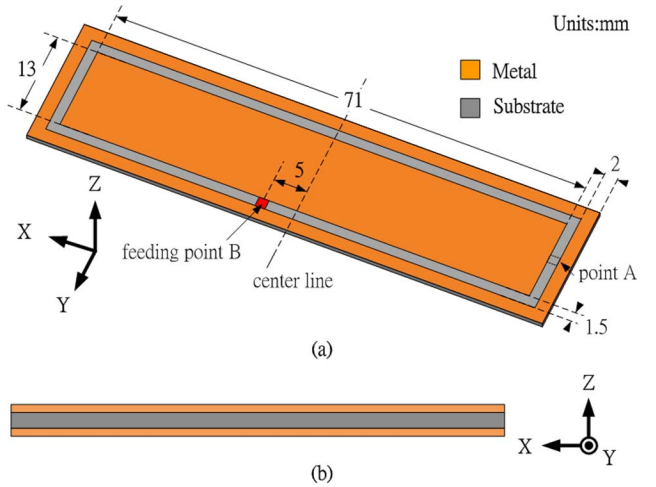

Fig. 1. Original rectangular adhesive-bandage-like antenna: (a) 3D view; and (b) side view.

B. Feeding Method

As shown in Fig. 1, two feeding points can be selected to excite the half-wavelength resonant mode of the main patch. The first feeding point excited the TM_{10} mode at Point A, and the second excited the TM_{01} mode at Point B. The electric field varied in half wavelengths across the length of the antenna, and the electric field was zero at the center of the patch and was maximized at the two sides. Therefore, it was more favorable to place the baseband or radio frequency (RF) circuits at the center of the patch. Moreover, the adhesive-bandage-like antenna was long and thin, making the input impedance approximately 2748 Ω along the two short edges. This meant that an additional matching network was required for Point A to match the antenna to 50 Ω. The feed point with 50 Ω of input impedance was near the center point of the long edge of the rectangular patch. Feeding Point B was 5 mm away from the center point, demonstrating superior impedance matching without requiring a matching circuit. The half-wavelength transverse-mode (TM_{01} mode) with a pattern maximum normal to the patch could be excited at Feeding Point B. Therefore, Feeding Point B was selected.

C. Characteristics of the Virtually Connected Ground Plane

A traditionally designed CPA consists of a patch surrounded by a closely spaced coplanar ground conductor and a back ground conductor [25], [26]. It has a large ground plane and requires an SMA connector to feed the antenna, which is inappropriate for circuit integration or for wearable applications. In the proposed design, the large coplanar side ground conductor was reduced to a 2-mm-thin rectangular metal ring, and the CPW feeding method was replaced by a gap source feed method. The rectangular metal ring could be treated as the ground plane, which was virtually connected to the large ground plane on the back owing to a large capacitance between

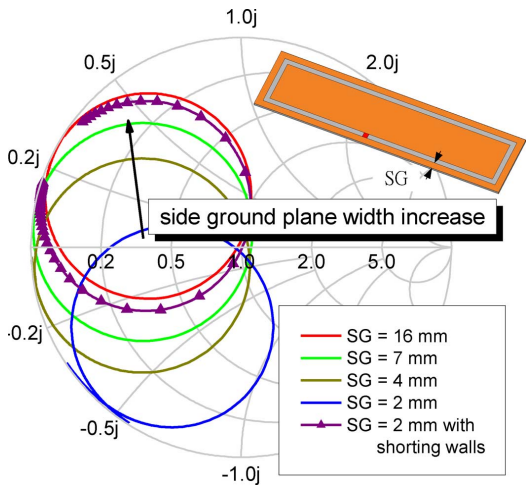

Fig. 2. Effects of various side ground plane widths (*SG*) on impedance characteristics. Reducing the side ground plane decreased the series capacitance of the proposed antenna.

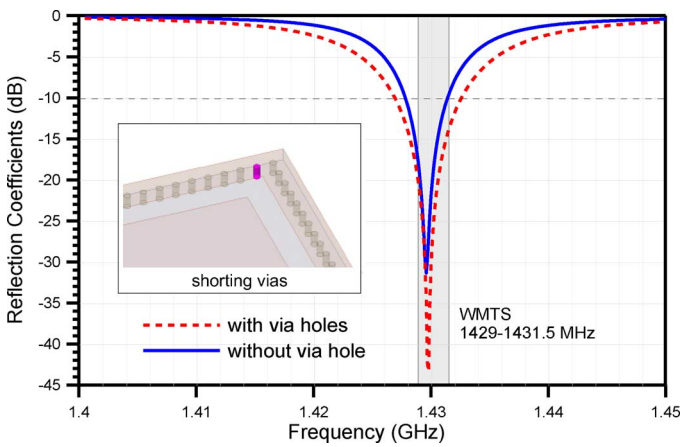

Fig. 3. Bandwidth produced by the adhesive-bandage-like antenna with and without shorting vias. The metal ring was 2 mm wide.

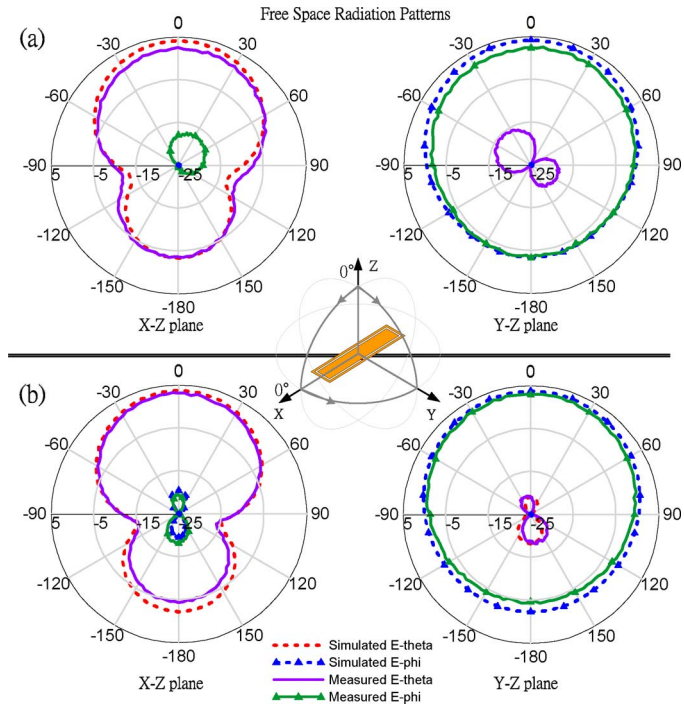

Fig. 4. The measured and simulated X-Z and Y-Z plane radiation patterns of the adhesive-bandage-like antenna in free space: (a) with shorting vias; and (b) without shorting vias.

TABLE I
COMPARISON OF THE MEASURED FREE SPACE ANTENNA PERFORMANCE OF THE ADHESIVE-BANDAGE-LIKE ANTENNA WITH AND WITHOUT VIAS

Design	With shorting vias	Without shorting vias
Frequency (GHz)	1.429	1.429
10-dB BW (MHz)	6.4	4.3
Peak Gain (dBi)	4.19	3.8
Radiation Efficiency (%)	75.7	75.87

the rectangular metal ring and the ground plane on the back. It has the same equivalent circuit as that of the patch antenna fed by a proximity-coupled feed [28]. By using this feeding scheme, the TM_{01} patch mode could be excited without the probe feeding scheme or the microstrip feeding scheme, which required a large area or a multilayer structure.

In this study, the effect of different ring widths was investigated. Commercial electromagnetic simulation software, HFSS, [29] based on the finite element method was used to model the proposed antenna. The simulated Smith chart with various side ground conductor widths is shown in Fig. 2. The figure shows that decreasing the ground plane reduced the series capacitance of the proposed antenna, therefore, the Smith chart moves toward the lower semicircular region. The effect of the proposed rectangular adhesive-bandage-like antenna with loaded vias connecting a 2-mm-wide rectangular metal ring to the ground conductor on the back was also examined. It contained 192 vias with a diameter of 0.42 mm, and the vias were spaced 1 mm apart. The Smith chart of the via-loaded adhesive-bandage-like antenna was similar to the Smith chart of the CPA with a wide ground conductor, which had a large series capacitance. In Fig. 3, a comparison of the simulated reflection coefficients of the proposed rectangular adhesive-bandage-like antenna with and without loaded vias is shown. The proposed design without loaded vias exhibited a smaller bandwidth than the via-loaded design did. When the width of the metal ring was reduced to 2 mm, the rectangular metal ring became part of the antenna, increasing the quality factor of the patch resonator and reducing the achieved bandwidth. WMTS require an operating bandwidth of only 4 MHz, therefore the design without loaded vias was selected to produce an antenna structure that was simple and flexible, even though the adhesive-bandage-like antenna with loaded vias demonstrated superior performance to the antenna that was not via loaded.

D. Antenna Mechanism Verification

The measured and simulated radiation patterns of the proposed rectangular adhesive-bandage-like antenna with and without loaded vias are shown in Fig. 4(a) and (b). No substantial changes were observed in the achieved peak gains and radiation patterns. A comparison of the measured antenna performance of the two antennas is shown in Table I.

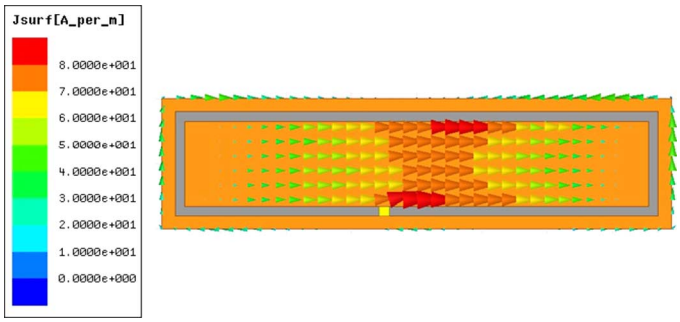

Fig. 5. Simulated vector surface current distribution during antenna operation in the TM_{01} mode.

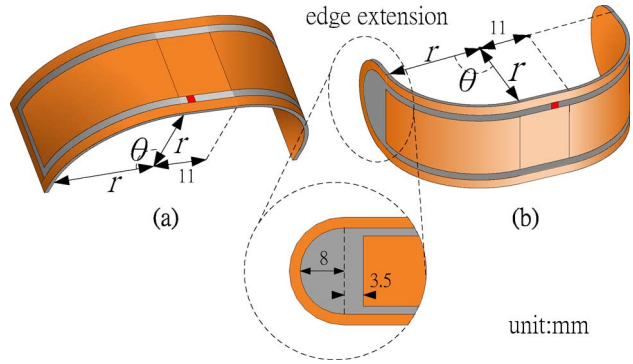

Fig. 6. Curved adhesive-bandage-like antenna: (a) original design; and (b) extended shielding ground conductor design.

The simulated current distribution at 1.4 GHz is shown in Fig. 5. The half-wavelength resonant mode was generated in the transverse direction. Placing baseband or RF circuits in the center of the main patch would fragment the patch, which would not change the overall radiation performance, but would shift the resonant frequency; therefore, the length of the rectangular patch must be redesigned if it is integrated with baseband or RF circuits. Similarly to a traditional microstrip antenna, two radiating slots contributed to the radiation on the broad side. The antenna gain achieved was relative to the length of the radiating slot. In this case, the width-to-length ratio was set to 5.46, and the measured antenna gain on the broad side was approximately 3.8 dBi. Polarization purity of the antenna was highly favorable on the broad side, which exhibited cross-polarization radiation that was approximately 25 dBi lower than the co-polarization radiation. In real wireless medical service applications, patients exhibit different postures; therefore the antenna exhibited a polarization mismatch, causing data reception problems. However, increasing the cross-polarized fields decreased the peak antenna gain of the wireless sensor node. Hence, the more favorable solution required a central processing unit with two quadrature linear polarized receiving antennas.

III. Antenna Deformation

To measure real-time ECG signals, a wearable sensor node is generally placed on the chest of a patient to provide optimal precision rates; in this case, the antenna is in its original planar shape. Adaptive antennas must be developed for other applications in the biomedical, military, and commercial fields. In [18], a curved zeroth-order resonant antenna was presented for WBAN applications. However, the measured peak gain of the antenna in free space was -7 dBi on the broad side, which is inadequate for applications that require wider transmission ranges. In addition to being used for breast-mounted sensors, the proposed antenna can be used in different applications because of its flexibility. This section describes the antenna performance of the proposed design after it was deformed into a curved shape. As shown in Fig. 6, the antenna was bent into an arc to evaluate the antenna performance. The simulation was performed using a simulation model with an antenna curvature radius of 20 mm.

The main obstacle to designing flexible antennas is that antenna performance factors, such as resonant frequency and radiation patterns, can be affected when the antenna changes shape. [30] and [31] examined the bending effect of a linear polarized patch antenna. Their results indicated that the resonant frequency shifted by approximately 1% when the E-plane was bent to nearly 90° (into a V-shape). The proposed adhesive-bandage-like antenna operated in the TM_{01} mode, thus, bending the antenna into the U-shape shown in Fig. 6(a) was classified as the E-plane bending category, slightly shifting the resonant frequency. However, the antenna radiation performance test demonstrated that as the proposed adhesive-bandage-like antenna was bent into a curved shape, the radiation pattern was directed to the back ($-z$), reducing the gain on the broad side ($+z$). The measured and simulated radiation patterns of the original design in the planar state are shown in Fig. 7(a). The radiation pattern was directed to the broad side with a measured gain of 3.8 dBi. When the antenna was bent into a curved shape (90°), the maximal gain of the antenna was directed to the back, as shown in Fig. 7(b). The measured gain on the back was 1.57 dBi, whereas it only decreased to -3.1 dBi on the broad side, indicating that the transmission quality of the antenna decreased when it was bent into a curved shape. This was caused by the finite ground plane and edge diffractions.

A modification to the antenna to improve the antenna gain and reduce the back radiation is shown in Fig. 6(b). The extension of the shield ground plane near the two radiating slots can be used to reduce the radiation on the back and maintain the maximal antenna gain on the broad side when the antenna is in free space and bent to 90°. The results of the parameter evaluation of the front-to-back ratio with various ground plane extension values are plotted in Fig. 8. As the length of the ground plane increased to 8 mm on each side, a favorable front-to-back ratio was achieved. The measured and simulated radiation patterns of the modified adhesive-bandage-like antenna when it was planar and bent into a curved shape (90°) are shown in Fig. 7(c) and (d), respectively. When the antenna was bent into a curved shape, the achieved antenna gain on the broad side measured 3.03 dBi, and the measured antenna gain on the back decreased to only -8.86 dBi, reflecting a favorable shielding result. Table II shows a summary of the measured results.

The effects of bending the original adhesive-bandage-like antenna design and the modified design with an extended shielding ground conductor are shown in Fig. 9. The figure presents the simulated antenna gain on the broad side when the two designs were bent at various angles. It shows that the broad side gain

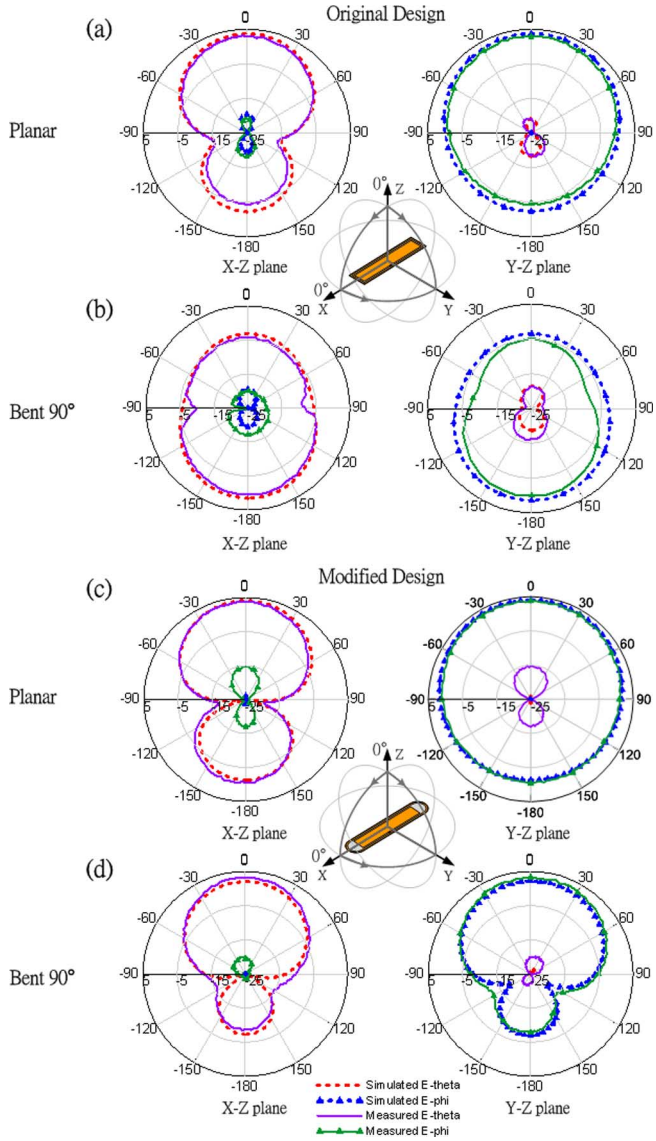

Fig. 7. Measured and simulated free space co-polarization and cross-polarization radiation patterns in the X-Z and Y-Z plane: (a) original design (planar shape); (b) extended shielding ground conductor design (planar shape); (c) original design (curved shape (90°)); and (d) extended shielding ground conductor design (curved shape (90°).

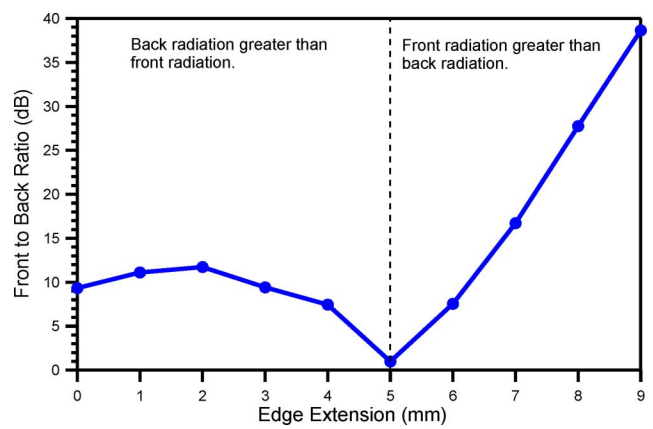

Fig. 8. Simulated front-to-back ratios with various edge extension values. The simulations were conducted with the antenna in free space and bent at 90°.

of the original design rapidly decreased with the bending angle, whereas the modified design maintained a favorable broad side

TABLE II
COMPARISON OF THE MEASURED RESULTS BETWEEN THE ORIGINAL ANTENNA AND THE MODIFIED DESIGN WITH AN 8 mm EDGE EXTENSION IN FREE SPACE

Design	Original		Modified	
	Planar	Banded	Planar	Banded
Frequency (GHz)	1.429	1.401	1.426	1.413
10-dB BW (MHz)	4.3	3.5	7.5	4.1
Peak Gain (dBi)	3.8	1.57	3.72	3.03
Efficiency (%)	75.87	51.8	89.5	35.7

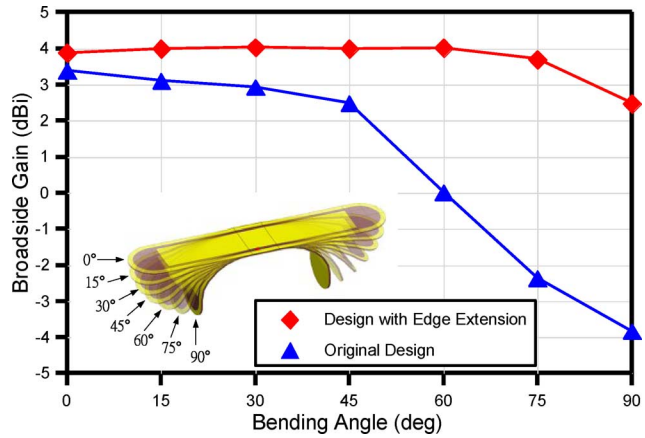

Fig. 9. Simulated broad side gain of the original adhesive-bandage-like antenna design (no edge extension) and the design with an 8 mm extended shielding ground conductor. Both designs were tested in free space.

gain when it was bent into a curved shape. The reactive near-fields of a small antenna can interact with the body [1], therefore, the on-body effect when the two designs were mounted on the tissue-equivalent phantom were investigated. A columnar phantom was used because the antenna was bent into a curved shape, as shown in Fig. 10. The tissue-equivalent phantom exhibited a relative permittivity $\varepsilon_r = 40.5$ and conductivity $\sigma = 1.2\ \mathrm{S/m}$ at 1.45 GHz [32]. The antennas and tissue-equivalent phantoms were spaced 1 mm apart. The simulation results showed that the modified design with the edge extension exhibited less frequency deviation ($\Delta f_{\mathrm{phantom}}/f_0$) when it was brought close to the tissue-equivalent phantom. The simulated broad side gains for the designs with and without the edge extension were 0.28 dBi and -3.04 dBi, respectively. The simulated radiation efficiency of the design with the edge extension was 34.7%, whereas the radiation efficiency of the original design was only 18.7%, which was attributed to the resonant frequency deviation. These results are listed in Table III, which are calculated at their free space resonant frequency when bent into curved shape.

IV. SAR Evaluation

Wearable devices for WBANs can be used to facilitate automatic medical treatment or remote monitoring of patient health. Medical telemetry devices are typically worn on the body of a patient, therefore, the safety of the human body is of a higher priority to these systems than it is to other wireless systems. The SAR must be considered to protect human tissue. The SAR of the proposed design was evaluated using a simulation model. A method for lowering the average SAR

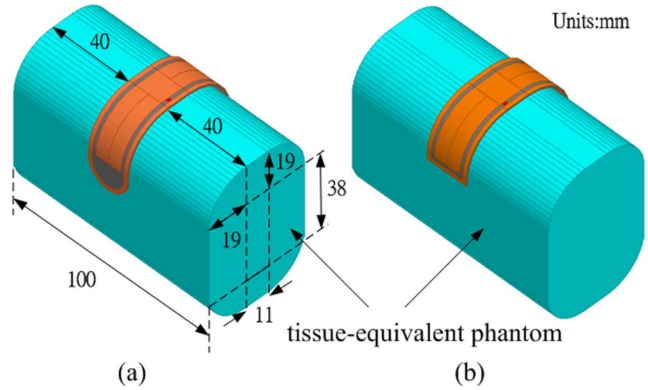

Fig. 10. Simulations showing the two designs bent at 90° and mounted on a tissue-equivalent phantom: (a) extended shielding ground conductor design; and (b) original design. The space between the antennas and phantoms was 1 mm.

TABLE III
SIMULATED ON-BODY EFFECTS OF THE TWO DESIGNS. THE RESULTS ARE CALCULATED AT THEIR FREE SPACE RESONANT FREQUENCY WHEN BENT INTO CURVED SHAPE. (1.413 GHz IS FOR THE DESIGN WITH EDGE EXTENSION AND 1.401 GHz IS FOR THE DESIGN WITHOUT EDGE EXTENSION)

Design	With edge extension	Without edge extension
Frequency Deviation	0.03%	0.2%
Broadside Gain	0.28 dBi	-3.04 dBi
Radiation Efficiency	34.7%	18.7%

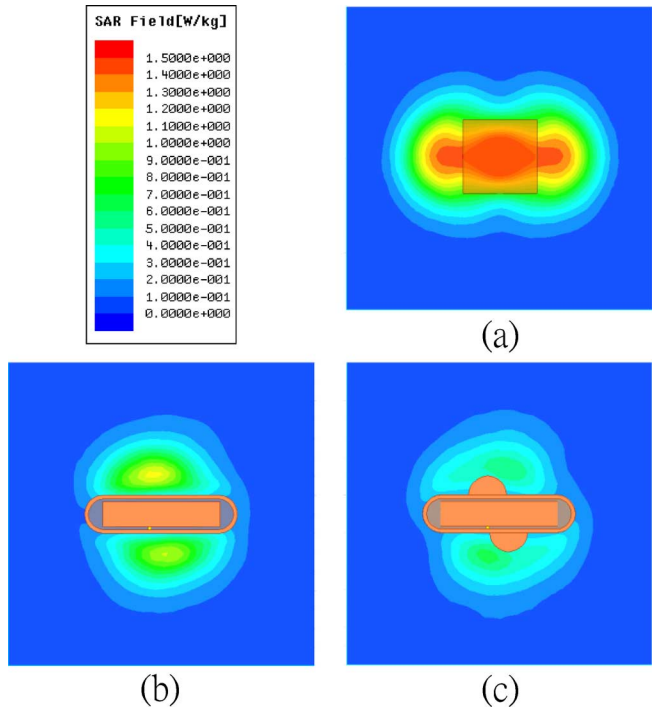

Fig. 11. Simulated average SAR distributions of: (a) a traditional half-wavelength square patch antenna; (b) the proposed adhesive-bandage-like antenna; and (c) the proposed adhesive-bandage-like antenna with two semicircles on the bottom ground plane. The antennas were located 1 mm above a flat phantom, with dimensions of 250 mm × 150 mm × 50 mm.

was also studied. In the simulation model, human tissue was modeled as a flat muscle-equivalent phantom with dimensions of 250 mm × 150 mm × 50 mm, and the antenna was located 1 mm above the tissue. The body tissue absorbs some radiated power, and the SAR value is relatively crucial to WBANs. For WBAN applications, devices are made as small as possible to facilitate wearability, and battery sizes are typically limited. Sensor devices must have extremely low power consumption to ensure that they can operate for long periods. Furthermore, their transmission ranges are typically designed to be no more than 3 m, therefore, the output power of the transmitter was set to -10 dBm, according to the link budget of the system [23]. The average SAR is shown in Fig. 11. The peak value of the calculated SAR at 1.465 GHz was 1.183 $\mathrm{W/kg^3}$, which is below the FCC restrictions. However, a method for lowering the SAR was also studied. The SAR field distribution is closely related to the shape of the antenna and its ground plane. As shown in Fig. 11(a), the SAR field distribution of a square patch antenna with a square ground plane exhibits a hot spot under the antenna. By contrast, the SAR field distribution of a patch antenna shaped like an adhesive bandage exhibits two hot spots near its two long sides, as shown in Fig. 11(b). To lower the peak value of the SAR field distribution, two semicircular metal segments were added to the bottom ground plane to disturb the electric field. As shown in Fig. 11(c), after adding the two semicircular metal segments, the SAR field became more uniform and the peak SAR value decreased by 45% from 1.183 W/kg3 to 0.65 $\mathrm{W/kg^3}$. Due to the offset feed of the antenna, the two semicircular segments had to be asymmetrically positioned to achieve a more favorable result. The adhesive-bandage-like antenna with the 8 mm extended shielding ground plane met the FCC SAR requirements. Therefore, the design with the two semicircles can be used as a reference design for a longer-range transmission application that requires a transmitter with a higher transmitting power.

V. ON-BODY EFFECTS AND EXPERIMENTAL RESULTS

The separation distance can vary with body movement or alternative applications; therefore, it is crucial to evaluate the antenna-tissue coupling and on-body performance. The simulated reflection coefficient results as a function of the antenna-phantom separation distance are shown in Fig. 12. A flat homogenous-tissue-equivalent phantom with dimensions of 250 mm × 150 mm × 50 mm was used for the simulation. The results indicated that the antenna only produced a slight deviation in the resonant frequency when it was in free-space and when it was placed in close proximity to the phantom. Radiation characteristic simulations were also performed, the results of which are listed in Table IV. The table shows that the simulated radiation efficiency was between 35% and 45% when the antenna was 0 mm to 9 mm away from the phantom, The simulated radiation efficiency was 83.7% when the antenna was in free space. A photograph of the realized adhesive-bandage-like antenna and the tissue-equivalent phantom is shown in Fig. 13. The phantom had dimensions of 250 mm × 150 mm × 50 mm as that of the simulation model. A 50 Ω semirigid coaxial cable was used to test the antenna. The semirigid coaxial cable had a center conductor diameter of 0.2 mm and an outer conductor diameter of 0.86 mm. The inner conductor was connected to the center patch, and the outer conductor was connected to the metal ring (virtual ground) on top of the circuit

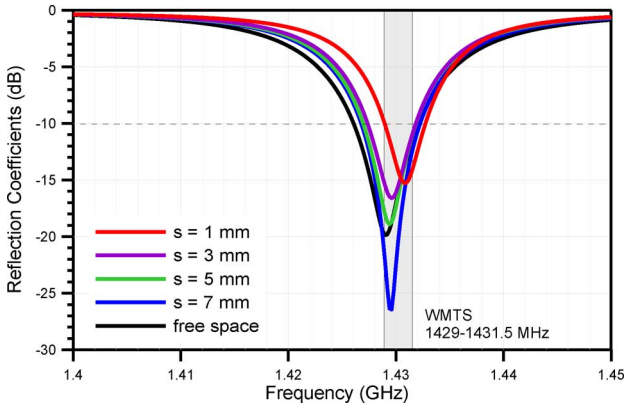

Fig. 12. Simulated reflection coefficient results as a function of antenna-phantom separation distance (s) for the planar antenna with edge extension.

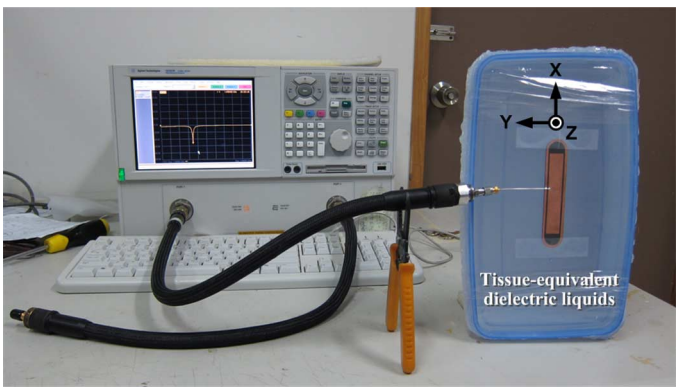

Fig. 13. Photograph of the proposed adhesive-bandage-like antenna. The tissue-equivalent phantom shown in the figure had dimensions of 250 mm × 150 mm × 50 mm.

TABLE IV
SIMULATED ANTENNA PERFORMANCE CHARACTERISTICS OF THE MODIFIED DESIGN AS A FUNCTION OF THE ANTENNA-PHANTOM SEPARATION DISTANCE

Antenna-phantom separation (mm)	**0**	**1**	**2**	**3**	**4**
Frequency (GHz)	1.431	1.4308	1.43	1.4296	1.4294
10-dB BW (MHz)	2.1	4	4	4.2	4.8
Peak Gain (dBi)	1.87	2.01	2.1	2.15	2.17
Radiation Efficiency (%)	35.4	41.7	42.3	42.3	42.4
Antenna-phantom separation (mm)	**5**	**6**	**7**	**8**	**9**
Frequency (GHz)	1.4294	1.4295	1.4296	1.4293	1.429
10-dB BW (MHz)	5	5.4	5.8	5.8	6.4
Peak Gain (dBi)	2.2	2.21	2.26	2.3	2.36
Radiation Efficiency (%)	42.5	42.8	43.1	43.7	44.6

board. The reflection coefficients were measured using an Agilent Network Analyzer, E8364B. In the experiment, the tissue-equivalent phantom—which was composed of a precise ratio of water, diethylene glycol monobuthyl ether (DGBE), and salt [32]—had the same properties and parameters as the described simulation model.

The reflection coefficients of the proposed antenna are shown in Fig. 14. The results were obtained from simulations and measurements of the antenna in free-space and on the tissue-equivalent phantom. The results are also listed in Table V for comparative purposes. The measured and simulated results were in favorable agreement. The measured results indicated that the impedance matching of the proposed adhesive-bandage-like antenna was insensitive to the presence of the body. A 10-dB bandwidth was measured from 1.429 GHz to 1.433 GHz, meeting the requirements of WMTS specifications.

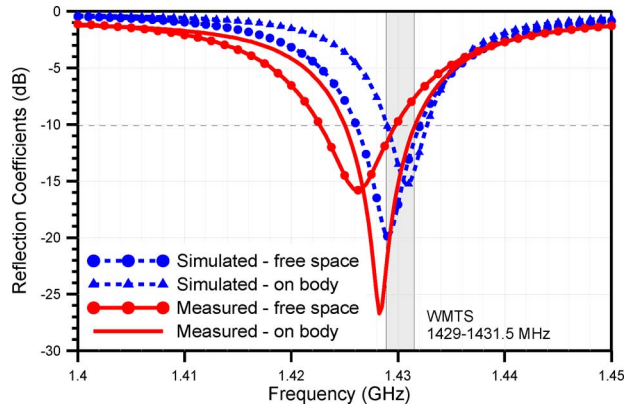

Fig. 14. Measured and simulated reflection coefficients of the proposed adhesive-bandage-like antenna when it was in free space and placed on the tissue-equivalent dielectric liquids.

TABLE V
SUMMARY OF THE SIMULATED AND MEASURED RESULTS FOR THE PROPOSED ANTENNA IN FREE-SPACE AND ON A PHANTOM

	Simulation		**Measurement**	
	Free space	On body	Free space	On body
Frequency (GHz)	1.429	1.43	1.426	1.428
10-dB BW (MHz)	6.2	4	7.5	7.05
Peak Gain (dBi)	3.91	2.01	3.72	0.8
Efficiency (%)	83.7	41.7	89.5	44.7

Radiation patterns, including those from the body-equivalent phantom, were also measured in an anechoic chamber. The measured and simulated radiation patterns of the proposed antenna when it was in a planar shape and mounted on the tissue-equivalent phantom are shown in Fig. 15. The measured and simulated peak gains on the broad side were approximately 0.8 dBi and 2.01 dBi, respectively. This decreased antenna gain can be attributed to the common mode current travel alongside the coaxial cable and the misalignment of the antenna under test (AUT). The polarization purity was favorable, and low amounts of cross-polarization radiation were observed. Human tissue is a lossy material, thus the tissue-equivalent phantom at the back of the antenna blocked some of the back radiation from the antenna, directing the radiation pattern to the broad side of the antenna. Some radiated power was absorbed by the tissue-equivalent phantom, decreasing the achieved antenna peak gain and radiation efficiency. The gain/directivity method was used to measure the antenna radiation efficiency [33], which was obtained from the far-field 3D radiation pattern, measured in an anechoic chamber. The measured radiation efficiency of the proposed adhesive-bandage-like antenna was 89.5% in free space and 44.7% when mounted on the tissue-equivalent phantom.

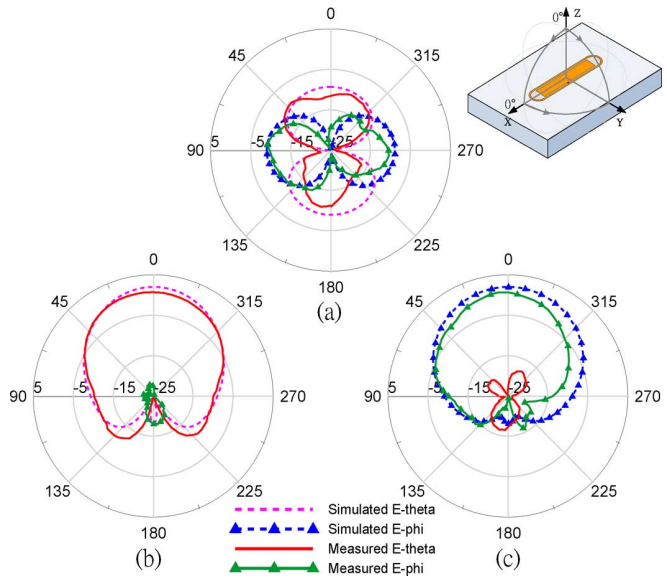

Fig. 15. Measured and simulated two-dimensional radiation patterns of the planar adhesive-bandage-like antenna on the tissue-equivalent phantom: (a) X-Y plane; (b) X-Z plane; and (c) Y-Z plane.

TABLE VI
SIMULATED EFFECTS OF TRUNK DIMENSIONS ON ANTENNA PERFORMANCE

Trunk Dimension (mm)	250 × 150 × 50	400 × 200 × 50
Resonant Frequency (GHz)	1.43	1.431
10-dB BW (MHz)	4	3.8
Peak Gain (dBi)	2.01	1.1
Radiation Efficiency (%)	41.7	39.9

The antenna and phantom were separated by 1 mm by the casing of the tissue-equivalent phantom. An RF-choke was applied when measuring the radiation pattern, which decreased the uncertainty caused by common mode errors produced by the gain/directivity method. There was agreement within 5%. In this study, the tissue-equivalent phantom exhibited dimensions of 250 mm × 150 mm × 50 mm. However, average trunk dimensions can vary by 400 to 550 mm × 150 to 200 mm × 50 to 100 mm, thus, the effect of various trunk dimensions were studied for comparison. The simulation results are listed in Table IV, which shows that the antenna peak gains were slightly different, but the resonant frequencies and radiation efficiencies were similar for the two trunk dimensions.

VI. CONCLUSION

This paper presents a novel adhesive-bandage-like antenna. The metal ring on top of the circuit board acted as a virtual ground, allowing the half-wavelength patch mode to be excited without requiring a complex feeding scheme. Therefore, the antenna was via-free and was capable of being bent into a curved shape. The antenna radiation characteristics when it was bent into a curved shape were studied. The proposed design can be used as a standalone antenna, or it can be integrated into a single-chip WMTS sensor. The antenna parameters, such as its reflection coefficients, SARs, radiation patterns, and radiation efficiencies, were also evaluated when it was placed on a tissue-equivalent phantom. The proposed adhesive-bandage-like antenna can be used to achieve a WBAN that performs effectively when placed on human tissue. The proposed antenna is compact, planar, and flexible, making it a favorable candidate for use in WBANs.

REFERENCES

[1] P. S. Hall *et al.*, "Antennas and propagation for on-body communication systems," *IEEE Antennas Propag. Mag.*, vol. 49, no. 3, pp. 41–58, 2007.
[2] P. S. Hall, Y. Hao, and K. Ito, "Guest editorial for the special issue on antennas and propagation on body-centric wireless communications," *IEEE Trans. Antennas Propag.*, vol. 57, no. 4, pp. 834–836, Apr. 2009.
[3] A. Alomainy, A. Sani, A. Rahman, J. G. Santas, and Y. Hao, "Transient characteristics of wearable antennas and radio propagation channels for ultrawideband body-centric wireless communications," *IEEE Trans. Antennas Propag.*, vol. 57, no. 4, pt. 1, pp. 875–884, Apr. 2009.
[4] L. Akhoondzadeh-Asl, P. S. Hall, and Y. Nechayev, "Novel conformal surface wave Yagi antenna for on-body communication channel," presented at the IEEE AP-S Int. Symp., Toronto, ON, Canada, Jul. 2010.
[5] H. R. Khaleel, H. M. Al-Rizzo, D. G. Rucker, and T. A. Elwi, "Wearable Yagi microstrip antenna for telemedicine applications," in *Proc. Radio and Wireless Symp.*, 2010, pp. 280–283.
[6] W. Xia, K. Saito, M. Takahashi, and K. Ito, "Performances of an implanted cavity slot antenna embedded in the human arm," *IEEE Trans. Antennas Propag.*, vol. 57, no. 4, pt. 1, pp. 894–899, Apr. 2009.
[7] N. Haga, K. Saito, M. Takahashi, and K. Ito, "Characteristics of cavity slot antenna for body-area networks," *IEEE Trans. Antennas Propag.*, vol. 57, no. 4, pp. 837–843, 2009.
[8] N. Chahat, M. Zhadobov, R. Sauleau, and K. Ito, "A compact UWB antenna for on-body applications," *IEEE Trans. Antennas Propag.*, vol. 59, no. 4, pp. 1123–1131, Apr. 2011.
[9] C.-H. Kang, S.-J. Wu, and J.-H. Tarng, "A novel folded UWB antenna for wireless body area network," *IEEE Trans. Antennas Propag.*, vol. 60, no. 2, pp. 1139–1142, Feb. 2012.
[10] M. Klemm and G. Troester, "Textile UWB antenna for wireless body area network," *IEEE Trans. Antennas Propag.*, vol. 54, no. 11, pp. 3192–3197, 2006.
[11] T. F. Kennedy, P. W. Fink, A. W. Chu, N. J. Champagne, G. Y. Lin, and M. A. Khayat, "Body-worn E-textile antennas: The good, the low-mass, and the conformal," *IEEE Trans. Antennas Propag.*, vol. 57, no. 4, pp. 910–918, Apr. 2009.
[12] S. Zhu and R. Langley, "Dual-band wearable textile antenna on an EBG Substrate," *IEEE Trans. Antennas Propag.*, vol. 57, no. 4, pp. 926–935, Apr. 2009.
[13] N. H. M. Rais, P. J. Soh, F. Malek, S. Ahmad, N. B. M. Hashim, and P. S. Hall, "A review of wearable antenna," in *Proc. Loughborough Antennas & Propagation Conf.*, Loughborough, U.K., pp. 225–228.
[14] Q. Bai and R. Langley, "Wearable EBG antenna bending and crumpling," in *Proc. Loughborough Antennas & Propagation Conf.*, Loughborough, U.K., Nov. 16–17, 2009, pp. 201–204.
[15] S.-J. Ha and C. W. Jung, "Reconfigurable beam steering using a microstrip patch antenna with a U-slot for wearable fabric applications," *IEEE Antennas Wireless Propag. Lett.*, vol. 10, pp. 1228–1231, 2011.
[16] E. K. Kaivanto, M. Berg, E. Salonen, and P. de Maagt, "Wearable circularly polarized antenna for personal satellite communication and navigation," *IEEE Trans. Antennas Propag.*, vol. 59, no. 12, pp. 4490–4496, Dec. 2011.
[17] T. J. Jung, J. H. Kwon, and S. Lim, "Flexible zeroth-order resonant antenna independent of substrate deformation," *Electron. Lett.*, vol. 46, pp. 740–742, 2010.
[18] J. Lee, S. I. Kwak, and S. Lim, "Wrist-wearable zeroth-order resonant antenna for wireless body area network applications," *Electron. Lett.*, vol. 47, pp. 431–433, 2011.
[19] C.-H. Lee, S.-Y. Chen, and P. Hsu, "Efficiency-enhanced and size-reduced coupled twin slots capacitively fed by conductor-backed coplanar waveguide," *IEEE Antennas Wireless Propag. Lett.*, vol. 8, pp. 1033–1035, 2009.
[20] T. Kellomaki, W. G. Whittow, J. Heikkinen, and L. Kettunen, "2.4 GHz plaster antennas for health monitoring," in *Proc. 3rd Eur. Conf. on Antennas and Propagation*, Berlin, Germany, Mar. 23–27, 2009, pp. 211–215.
[21] T. Kellomaki and W. Whittow, "Bendable plaster antenna for 2.45 GHz applications," in *Proc. Loughborough Antennas Propagation Conf.*, Loughborough, Nov. 2009, pp. 453–456.

[22] A. W. Astrin, H.-B. Li, and R. Kohno, "Standardization for body area networks," *IEICE Trans. Commun.*, vol. E92-B, no. 2, pp. 366–372, Feb. 2009.
[23] J.-Y. Yu, W.-C. Liao, and C.-Y. Lee, "A MT-CDMA based wireless body area network for ubiquitous healthcare monitoring," in *Proc. BioCAS*, Nov. 2006, pp. 98–101.
[24] J. Yoo, L. Yan, S. Lee, H. Kim, B. Kim, and H.-J. Yoo, "An attachable ECG sensor bandage with planar-fashionable circuit board," in *Proc. Int. Symp. on Wearable Computers*, 2009, pp. 145–146.
[25] L. Giauffert, J. Laheurte, and A. Papiernik, "Study of various shapes of the coupling slot in CPW-fed microstrip antennas," *IEEE Trans. Antennas Propag.*, vol. 45, no. 4, pp. 642–647, Apr. 1997.
[26] K. Li, C. H. Cheng, T. Matsui, and M. Izutsu, "Simulation and experimental study on coplanar patch and array antennas," in *Proc. Asia-Pacific Microwave Conf.*, Sydney, NSW, Dec. 2000, pp. 1411–1414.
[27] K. Li, C. H. Cheng, T. Matsui, and M. Izutsu, "Coplanar patch antennas: Principle, simulation and experiment," in *Proc. IEEE AP-Symp.*, 2001, vol. 3, pp. 402–405.
[28] R. Garg, P. Bhartia, I. Bahl, and A. Ittipiboon, *Microstrip Antenna Design Handbook*. Norwood, MA, USA: Artech House, 2001.
[29] ANSYS HFSS Ver. 13 ANSYS Corporation.
[30] M. Tanaka and J. H. Jang, "Wearable microstrip antenna," presented at the IEEE AP-S Int. Symp. on Antennas and Propagation and URSI North Amer. Radio Science Meeting, Columbus, OH, USA, Jun. 2003.
[31] J. S. Dahele, R. J. Mitchell, K. M. Luk, and K. F. Lee, "Effect of curvature on characteristic of rectangular patch antenna," *Electron. Lett.*, vol. 23, pp. 74–749, Jul. 1987.
[32] K. Fukunaga, S. Watanabe, Y. Yamanaka, H. Asou, Y. Ishii, and K. Sato, "Optimisation of tissue-equivalent liquids for SAR measurements," in *Proc. Progress in Electromagnetic Research Symp.*, Pisa, Italy, Mar. 28–31, 2004, pp. 65–68.
[33] C. A. Balanis, *Antenna Theory: Analysis and Design*. New York, NY, USA: Harper and Row, 1982.

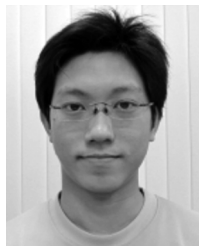

Yu-Jen Chi (S'13) was born in Taipei, Taiwan, R.O.C., in 1985. He received the B.S. and M.S. degrees in electronic engineering from National Ilan University, I-Lan, Taiwan, R.O.C., in 2007 and 2009, respectively. He is currently working toward the Ph.D. degree at National Chiao Tung University, Hsinchu, Taiwan, R.O.C.

His main research interests are in multiband antennas for mobile devices, CRLH leaky wave antennas, millimeter-wave antennas, metamaterials, and antennas for biomedical applications.

Mr. Chi received the Best Poster Award in the 2009 IEEE International Workshop on Antenna Technology (iWAT 2009).

Fu-Chiarng Chen (M'11) received the B.S. and M.S. degrees from the National Taiwan University, Taipei, Taiwan, R.O.C., in 1988 and 1990, respectively, and the Ph.D. degree from the University of Illinois at Urbana-Champaign, Champaign, IL, USA, in 1998, all in electrical engineering.

In 1998, he joined the Qualcomm Incorporated, San Diego, CA, USA. From 2003 to 2007, he was an Assistant Professor with the Department of Electrical Engineering, National Chiao Tung University, Hsinchu, Taiwan, where he is now an Associate Professor. His research interests include the experimental and computational aspects of applied electromagnetics, antennas, radars, inverse scattering, and RF/Microwave engineering for wireless communications. He holds eight U.S. patents.

Dr. Chen won the First Place Prize in the 1998 IEEE Antennas and Propagation Society International Symposium Student Paper Competition. He received the Macronix Young Chair Professorship Award in 2005, the National Chiao Tung University Outstanding Researchers Award in 2007 and 2008, the National Chiao Tung University Excellent Teaching Award in 2008, the National Chiao Tung University Electrical and Computer Engineering College Excellent Teaching Award in 2011 and 2012, and the National Chiao Tung University Excellent Mentoring Award in 2008 and 2011.